A dual lake approach reveals the impact of Holocene oxygen availability and climate on molecular proxy records in the sub-Arctic

David J. Harning[1]*, Samuel Sacco[2], Jonathan H. Raberg[1,3], Nicolò Ardenghi[1], Julio Sepúlveda[1,4], Beth Shapiro[2], Gifford H. Miller[1,4], Áslaug Geirsdóttir[5]

1 Institute of Arctic and Alpine Research, University of Colorado, Boulder, CO, USA
2 Department of Ecology and Evolutionary Biology, University of California, Santa Cruz, CA, USA
3 Department of Geology and Geophysics, University of Wyoming, Laramie, WY, USA
4 Department of Geological Sciences, University of Colorado, Boulder, CO, USA
5 Faculty of Earth Sciences, University of Iceland, Reykjavík, Iceland
* Corresponding author: David J. Harning (david.harning@colorado.edu)

This paper is a non-peer reviewed preprint submitted to EarthArXiv. It will be updated as the manuscript progresses through peer review.

Abstract

Ancient DNA and branched glycerol dialkyl glycerol tetraethers (brGDGTs) are new, powerful tools to reconstruct past ecosystems and climate in high-latitude lakes, but often require contrasting oxygen conditions for reliable interpretations. Here, we present a new approach using adjacent oxic and anoxic lakes to 1) better understand how redox potential impacts these proxies using isoprenoid GDGTs, and 2) reconstruct holistic changes in climate, human settlement, and plant history. We observe, first, that oxic lakes are likely to yield more reliable brGDGT-based paleotemperature records. Second, while anoxic lakes are optimal for ancient DNA preservation, commonly studied shallow lakes are more susceptible to past changes in oxygen availability that can lead to fragmentary DNA records. Finally, our dual lake approach highlights that climate, and not humans, has been the primary forcing behind Holocene vegetation changes in northeast Iceland, and therefore provides ideal constraints for earth system models.

Introduction

Modern anthropogenic warming and enhanced moisture availability are reshaping high-latitude plant communities with important consequences for the climate system and regional biodiversity (*1, 2*). These changes include the northward expansion and increased height and density of woody vegetation (*3, 4*), which reduce surface albedo (*5*) and increase atmospheric water vapor (*6*), further amplifying high latitude warming (*7*). Changes in tundra ecosystems will also leave lasting impacts on regional biodiversity, food web structure, and nutrient availability (*4, 8, 9*). Plant records from warm periods in Earth's history can provide fundamental insight into the processes that may be expected in our near future and help constrain predictive models (*10, 11*). Some high-latitude regions, such as Iceland, offer the opportunity to examine the natural relationship between Holocene changes in climate and plants as humans only colonized Iceland ~1080 years before present (BP, *Landnámabók*). Geologic records that cover the settlement of Iceland also allow us to better understand the impact of pastoral activities on sensitive landscapes (*12*). To this end, recent efforts have targeted high-resolution lake sedimentary records in Iceland (*13-15*), but open questions remain on the evolution of Holocene plant communities as well as the relative impact of climate and humans on the landscape (*12*).

Recent analytical advances provide new molecular tools to quantify changes in past temperature, plant communities, and human presence using lipid biomarkers and

sedimentary ancient DNA (*sed*aDNA) in lake sediment. For lipids, the methylation number of branched glycerol dialkyl glycerol tetraethers (brGDGTs), a globally ubiquitous bacterial lipid, shows strong empirical correlations to warm season temperatures in high-latitude lakes (*16, 17*). For plant histories, *sed*aDNA metabarcoding provides more reliable and continuous records compared to other traditional proxies (i.e., pollen and macrofossils) due to its local source in lake catchments and generally good preservation in sediments (*18-20*). Similarly, mammalian *sed*aDNA provides evidence for the presence of taxa, including those associated with animal husbandry (*21-23*). However, brGDGT production and *sed*aDNA preservation may be influenced by other lake processes, including oxygen availability (e.g., *24, 25*), which is important to consider for high latitude lakes that have a wide range of mixing and oxygen dynamics (*26*). While the impact of oxygen histories can be inferred from several geochemical tools, such as archaeal isoprenoid GDGTs (isoGDGTs) as a proxy for methanogenesis (e.g., *27, 28*), oxygen availability is rarely considered in paleoclimate studies.

In this study, we address these shortcomings in a natural laboratory experiment by comparing detailed multi-proxy paleoclimate records from two neighboring lakes in Iceland (separated by 0.6 km and at similar elevation, Fig. 1). Due to different lake morphometries (large and deep vs small and shallow), the two lakes feature contrasting amounts of dissolved oxygen, and the lakes' proximity means that climate is held as a constant. Relying on a suite of molecular proxies, including brGDGTs for temperature, *sed*aDNA for plant and mammal history, and isoGDGTs for oxygen availability, we answer the following questions. First, how does lake morphometry and oxygen availability impact the fidelity of widely used brGDGT and *sed*aDNA proxies through time? Second, how can sediment records from morphologically contrasting lakes lead to more holistic paleoenvironmental reconstructions than from one site alone? Ultimately, our dual lake approach provides a model for overcoming the limitations of oxygen availability when using molecular proxies in Arctic lakes and new insight into high-latitude climate-driven ecosystem changes.

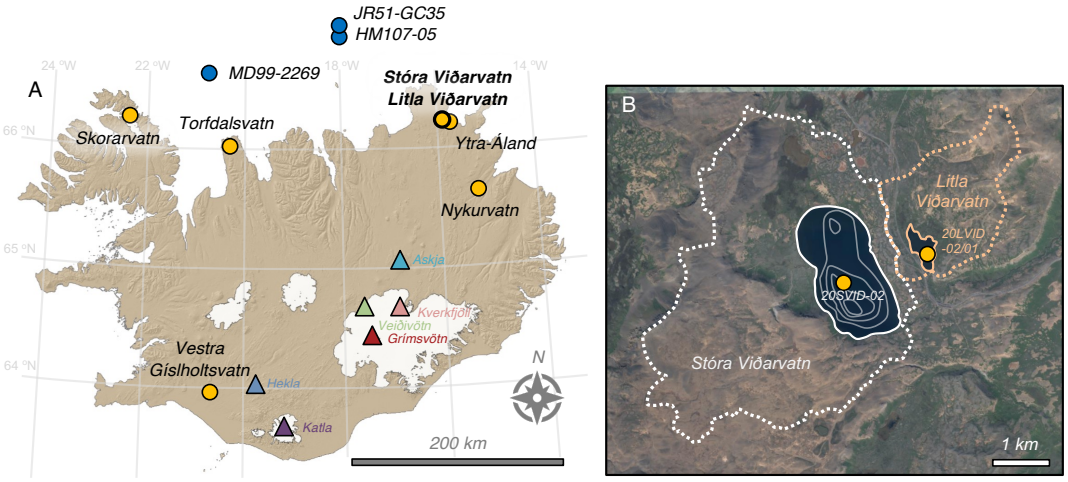

Fig. 1. Overview map of Iceland. (**A**) Locations of Stóra and Litla Viðarvatn in northeast Iceland related to other terrestrial (yellow) and marine (blue) paleoclimate record sites. Central volcanos (triangles) that produced tephra layers used in age models are also marked. (**B**) Close-up of Stóra and Litla Viðarvatn, their catchments (dotted lines), bathymetry (10-m isolines), and location of core sites for 20SVID-02 (*14, 30*) and 20LVID-02/01 (this study). 2017 base image courtesy of Loftmyndir ehf.

Results

Modern seasonal lake stratification and oxygen availability

iButton temperature loggers deployed from September 2019 to 2020 record seasonal fluctuations in lake water temperature in the two lakes, Stóra and Litla Viðarvatn (Fig. 2A-B). Due to the different lake volumes and energy required to heat water, peak summer temperature in Litla Viðarvatn (June, 14.7 ºC) is earlier and higher than in Stóra Viðarvatn (August, 10.6 ºC). In both lakes, water temperature begins to increase in May, reflecting the seasonal melting of lake ice and overturning of the lake water columns. Surface and bottom water temperatures at Stóra Viðarvatn's sediment coring location show minimal thermal stratification during summer and winter months. This is supported by vertically homogenous water quality measurements (i.e., dissolved oxygen, specific conductivity, and pH) (*29*) taken in September 2019 and February 2020 (Fig. 2C and S1). However, the same water quality measurements for Litla Viðarvatn show the development of seasonal stratification in February 2020 (Fig. 2D and S1), reflected by lower bottom water dissolved oxygen concentrations (Fig. 2D).

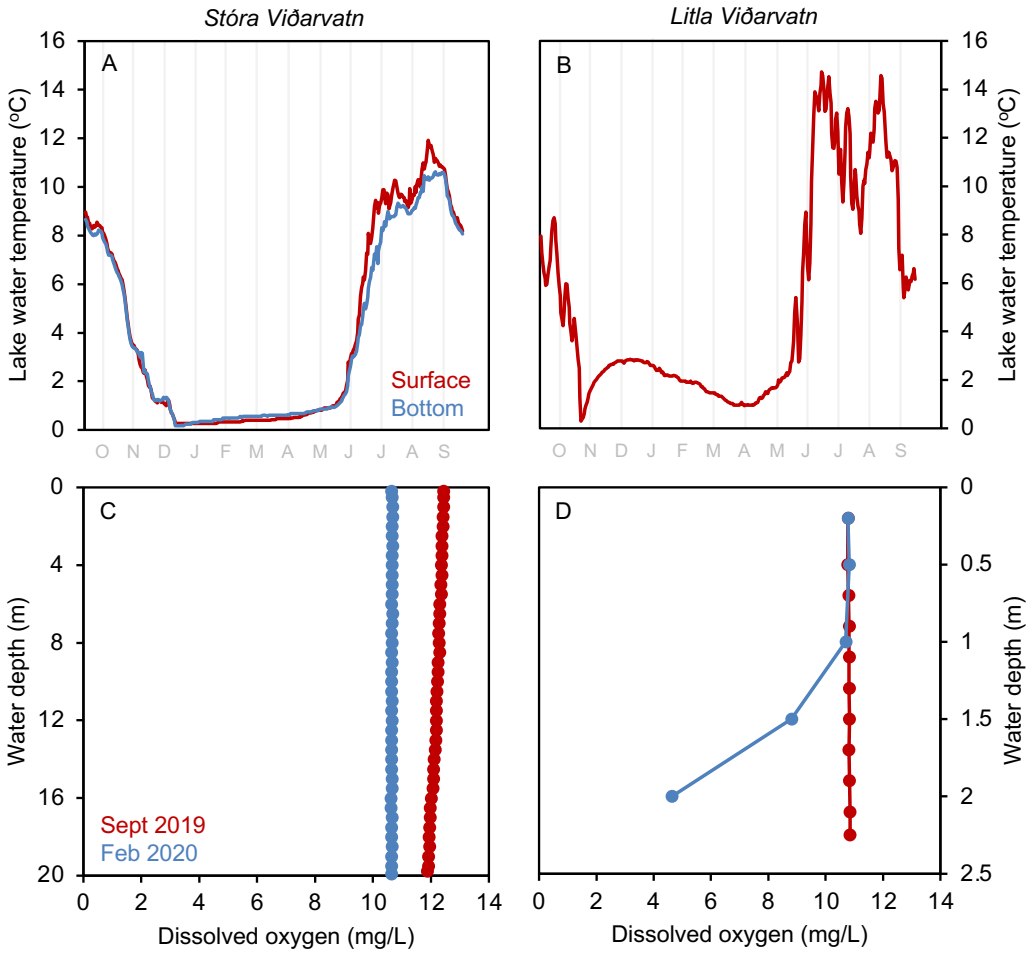

Fig. 2. Modern water quality measurements for Stóra Viðarvatn (left) and Litla Viðarvatn (right). (**A-B**) iButton temperature measurements from September 2019 to September 2020 for surface (red) and bottom water (blue) (*16*) and (**C-D**) Sonde dissolved oxygen concentrations (mg/L) from September 2019 (red) and February 2020 (blue) (*29*). See supplemental Fig. S1 for seasonal pH and specific conductivity Sonde measurements.

Lake sediment age models

Sediment core images from Stóra and Litla Viðarvatn demonstrate similar stratigraphies, including visible tephra layers of known age (Fig. S2). Based on tephra geochemical analyses in Stóra Viðarvatn (*14, 30*), we use the relatively thick and black G10ka Series (10400 to 9900 BP) (*31*) and light gray Hekla 3 tephra layers (Hekla 3, 3010 ± 54) (*32*) in Litla Viðarvatn's age model (Fig. 3B, Table S1). Bayesian age models for both lake sediment records show relatively linear sedimentation rates throughout the Holocene, although there is slightly more variability in Litla Viðarvatn, possibly due to the lake's smaller size and susceptibility to changes in sediment supply (Fig. 3). Stóra Viðarvatn's record spans the last 10950 years BP (Fig. 3A) (*30*) and Litla Viðarvatn's record spans the last 9900 years BP (Fig. 3B). Both age models feature a high density of chronological control points, including common tephra layers (Fig. 3), allowing for high-resolution and synchronized proxy record comparisons between the two lakes.

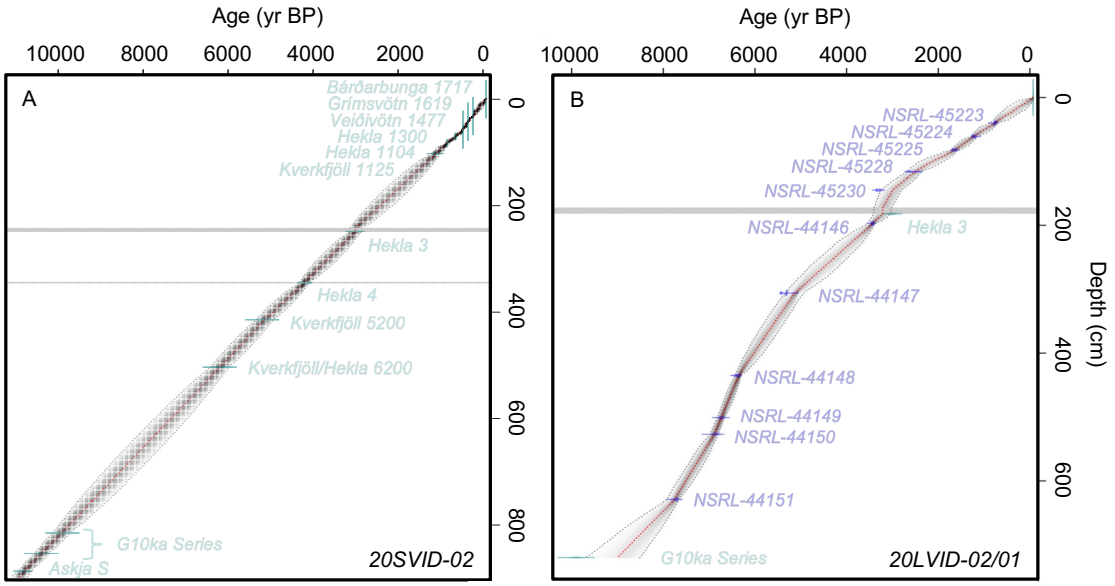

Fig. 3. Bayesian age models for (A) Stóra Viðarvatn and (B) Litla Viðarvatn. Age models constructed using tephra layers of known age (green) and radiocarbon dates of plant macrofossils (blue) using the R package rbacon, default model functions (*70*), and the IntCal20 calibration curve (*71*). The solid red line reflects the median of model iterations, and the outer gray lines reflect the 95% confidence envelope. Horizontal gray bars indicate periods of instantaneous tephra layer deposition. See Table S1 for radiocarbon information.

Lake sediment organic matter sources

Holocene magnetic susceptibility (MS) records are similar, showing relatively high values near the base of each record and then relatively low values until increases beginning at 1150 BP in Stóra Viðarvatn and and 1400 BP in Litla Viðarvatn (Fig. 4A-B), where higher MS values generally reflect the greater contribution of minerogenic material to the lake sediment. Decadal-scale MS spikes are due to tephra layers. Bulk organic geochemistry in Litla Viðarvatn is characterized by %TOC ranges from 0.19 to 10.7 %, C/N ranges from 3.86 to 11.0, $\delta^{13}C$ ranges from -34.9 to -19.4 ‰, and BSi ranges from 21 to 128 FTIRs absorbance units (Fig. 4). In comparison to Stóra Viðarvatn's bulk organic geochemistry (*14*), Litla Viðarvatn's generally higher %TOC (Fig. 4C-D), higher C/N values (Fig. 4E-F), and more enriched $\delta^{13}C$ values (Fig. 4G-H) reflect a more productive system with greater terrestrial and aquatic organic matter preserved in the sedimentary record (e.g., *12*). Finally,

both lakes feature similar BSi records indicating relatively similar responses of diatom productivity through time (e.g., *33*). In both cases, the most notable BSi changes are persistent shifts to lower values beginning at 1800 BP and 1700 BP in Stóra and Litla Viðarvatn, respectively (Fig. 4I-J).

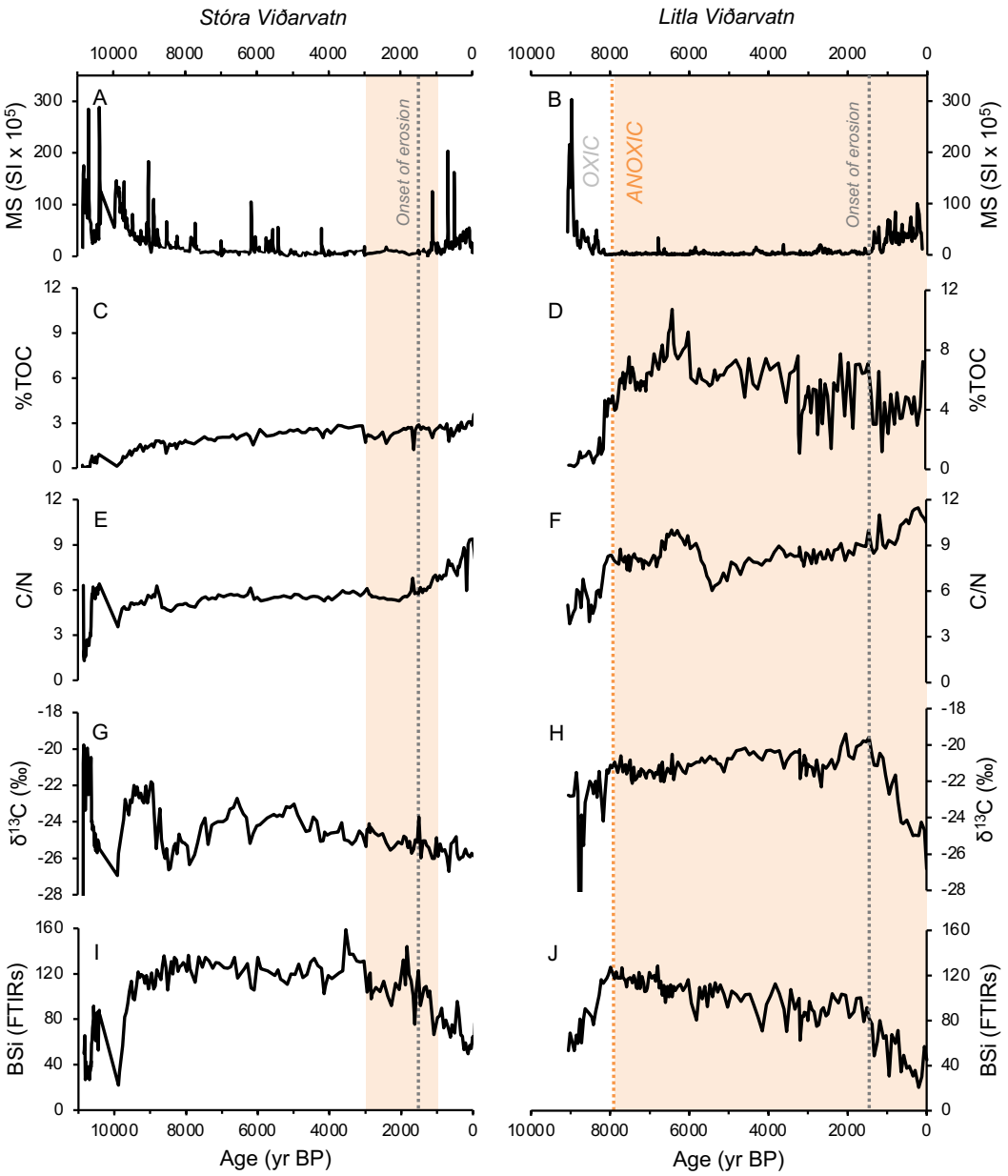

Fig. 4. Bulk geochemistry proxy data from Stóra Viðarvatn (left) and Litla Viðarvatn (right). Orange bars reflect portions of the sediment cores likely impacted by low oxygen lake conditions based on isoGDGT-0/crenarchaeol ratios (see Fig. 5A-B). Vertical gray dashed line reflects the onset of soil erosion in both lakes at ~1500 BP.

GDGT-inferred oxygen availability and temperature

Isoprenoid and branched GDGTs are present above the detection limit in all samples from Stóra and Litla Viðarvatn. The ratio of isoGDGT-0/crenarchaeol range from 0.88 to 75.6 in Stóra Viðarvatn and from 1.20 to 380 in Litla Viðarvatn (Fig. 5A-B). Stóra Viðarvatn‘s isoGDGT-0/crenarchaeol ratio remains low (<10) for most of the record with a temporary but sustained increase identified between 2900 and 1000 BP (Fig. 5A). In contrast, Litla

Viðarvatn's isoGDGT-0/crenarchaeol ratio remains elevated from 8000 BP onwards (Fig. 5B). Increased isoGDGT-0/crenarchaeol ratios likely indicate intervals of more reducing conditions (low oxygen) that promoted archaeal methanogens (*27, 34*).

In Stóra and Litla Viðarvatn sediments, the distributions of brGDGTs are distinct (Fig. S3A). When compared to those of modern Icelandic lake and soil samples, the distribution patterns suggest that brGDGTs in Stóra Viðarvatn are generally derived from sources in the lake while brGDGTs in Litla Viðarvatn may be sourced more from catchment soils (Fig. S3A). In terms of temperature proxies, relative MBT'$_{5Me}$ ratios (Fig. 5E-F) (*35*) and quantitative months above freezing (MAF) indices are relatively flat in both Stóra and Litla Viðarvatn (Fig. 5G-H) (*16, 17*). However, mean summer temperature (MST) anomalies differ between the two lakes (Fig. 5I-J) (*36*). MST anomalies from Stóra Viðarvatn show relatively high yet variable temperatures until 5600 BP, after which temperatures generally decline towards present. For Litla Viðarvatn, the highest MST anomalies are reached during the earliest portion of the record between 8700 and 8150 BP, before declining rapidly and fluctuating between ~0 and 1 ºC relative to today for the remainder of the record (Fig. 5I-J).

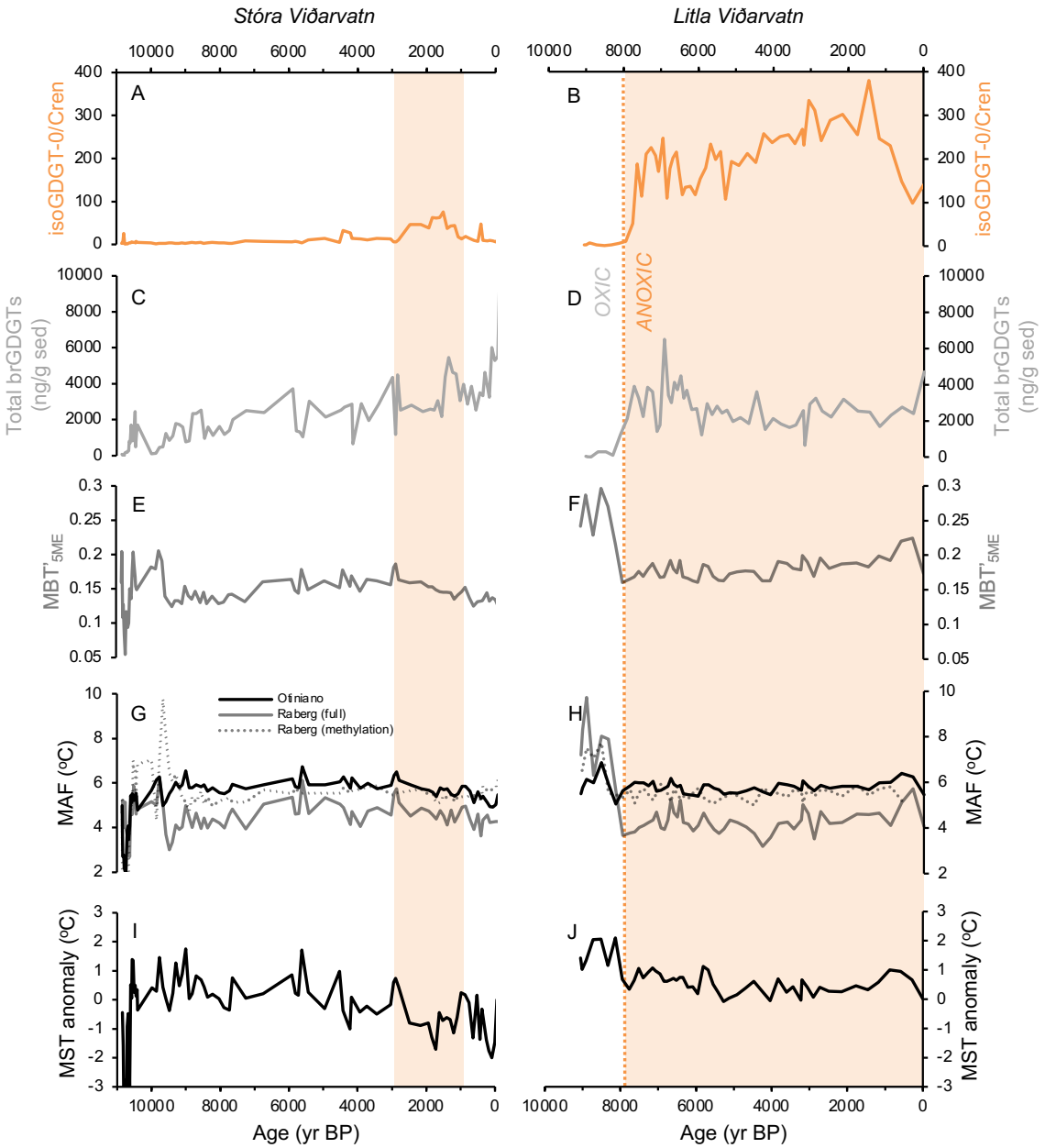

Fig. 5. Isoprenoid GDGT and brGDGT proxy records from Stóra Viðarvatn (left) and Litla Viðarvatn (right). Orange bars reflect portions of the sediment cores likely impacted by low oxygen lake conditions based on isoGDGT-0/crenarchaeol ratios (**A-B**). MBT'$_{5ME}$ after De Jonge et al. (2014), MAF after Raberg et al. (2021) and Otiniano et al. (2024), and MST anomaly after Harning et al. (2020).

Plant and mammalian sedaDNA

Of the 54 samples analyzed in Litla Viðarvatn, 47 yield amplifiable plant DNA using the *trnL* P6 loop primer set (*37*, see *ref 30* for Stóra Viðarvatn details). The 7 samples that failed were the samples older than 8000 BP. Following data filtering, the *trnL* dataset yields 8,147,575 total assigned reads, with an average of 150,881 assigned reads per sample. The relative stability of qPCR cycle threshold (C_T) values, which reflect PCR efficiency and the quantity of suitable target sequences for amplification, reveal relatively stable trends and indicate that the efficiency of PCR amplification of trnL targets is consistent throughout the record (Fig. S4). Metabarcoding technical quality (MTQ) and analytical quality (MAQ)

scores are below suggested low quality thresholds (0.75 and 0.1, respectively) (*38*) in some samples during the Early and Middle Holocene (Fig. S4). However, given that the quality scores correlate with species richness and species richness is always below 30 (Fig. S4), the low MTQ and MAQ scores are likely an artifact of the requirement that the 10 best represented barcode sequences are required for calculation (*38*), and not necessarily an indication of poor DNA preservation. However, the low MTQ and MAQ scores for the oldest 7 samples likely do reflect poor DNA preservation as amplification of trnL targets resulted in no assigned reads. We identified 47 plant taxa across a range of plant functional groups throughout Litla Viðarvatn's lake sediment record, and except for aquatic plants, species richness generally increases throughout the Holocene in all plant functional groups (Fig. 6). Compared to Stóra Viðarvatn, Litla Viðarvatn has a higher richness of aquatic plants (Fig. 6).

For mammalian DNA, we experimented with several primers and approaches targeting mammals, including sheep – the most populous domesticated mammal in Iceland (*39*) – in a subset of Late Holocene sediment samples from both lakes (see Supplemental Materials). Results using the mammP007 primer, which is commonly used to identify the presence of sheep in lake sediment records (e.g., *22*), failed to yield any positive identification of sheep or any other domesticated mammals in Stóra and Litla Viðarvatn. However, we did detect sheep in 5/5 replicates using mammP007 in two modern samples (lake surface sediment and soil) from Vestra Gíslholtsvatn, a lake in southwest Iceland with large modern sheep populations (Fig. 1A). Broadly, the other mammalian primer (16Smamm) (*40*), sheep-specific primers (L15496 forward primer and H15661 reverse primer) (*41*), and hybridization capture approaches tested also failed to yield identification of mammals in the lake sediment samples. As sheep are present in the catchments of both lakes today, these results imply that the density of domesticated mammal populations around Stóra and Litla Viðarvatn has been too low to leave a *sed*aDNA signal.

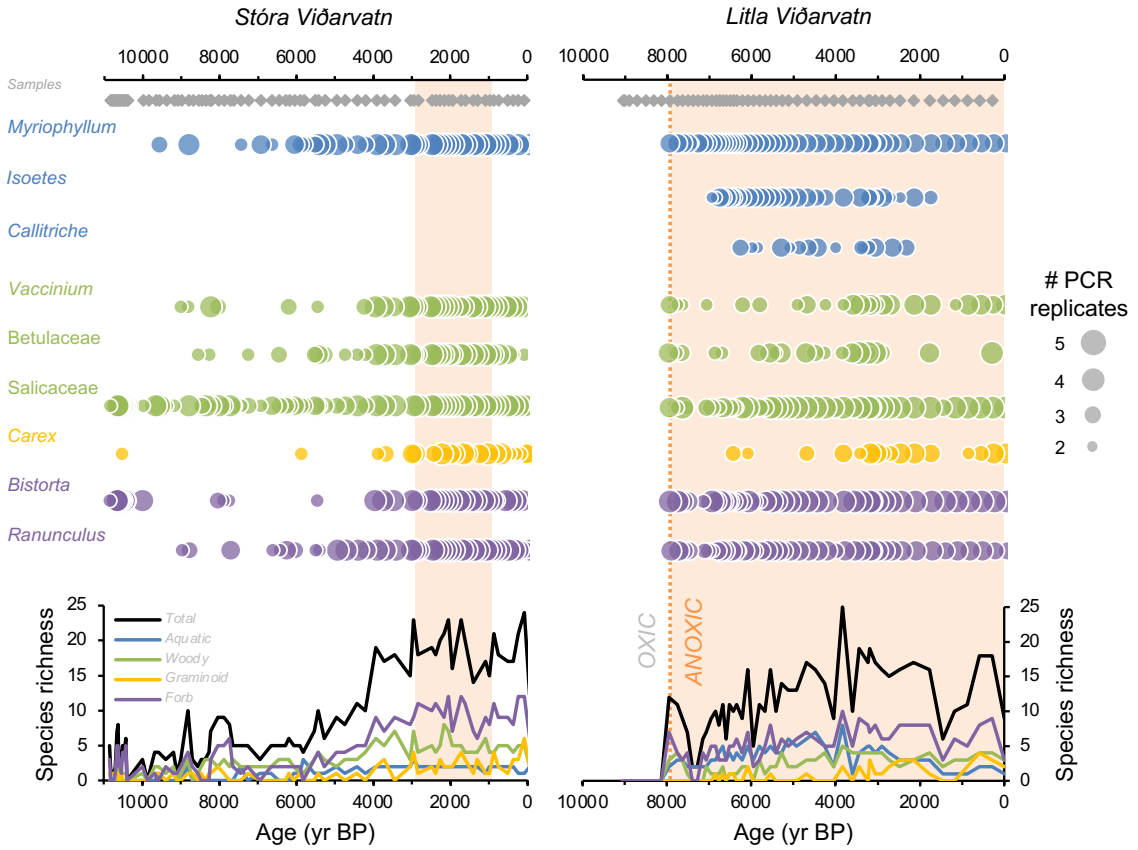

Fig. 6. Plant *sed*aDNA records from Stóra Viðarvatn (left) and Litla Viðarvatn (right). Top: gray diamonds denote where samples were taken and analyzed for DNA metabarcoding. Bubble plots reflect the presence/absence of select taxa, where the size of the bubble is proportional to the number of PCR replicates (1-5). Bottom: species richness shown for the total number of taxa as well as four plant functional groups (i.e., aquatic, woody, graminoid, and forb). Orange bars reflect portions of the sediment cores likely impacted by low oxygen lake conditions based on isoGDGT-0/crenarchaeol ratios (see Fig. 5A-B).

Discussion

Lake and catchment morphometries

Stóra and Litla Viðarvatn differ substantially in maximum lake depth (48 vs 2.5 m), surface area (2.51 vs 0.21 km^2), and catchment area (16.6 vs 1.96 km^2) (Fig. 1B), which lead to distinct seasonal changes in the physical-chemical properties of the lakes. While Stóra Viðarvatn‘s sediment core and water property measurements were not taken from the deepest portion of the lake, which is located to the south (Fig. 1B), measurements taken at 20 m water depth indicate that the lake remains well mixed even at greater depths throughout the year (Figs. 2A and 2C). In contrast, shallow Litla Viðarvatn develops an oxycline during winter, leading to the seasonal depletion of dissolved oxygen in its bottom water (Fig. 2D). We hypothesize that Litla Viðarvatn‘s oxycline results from its comparatively smaller volume, where dissolved oxygen is more readily depleted during microbial respiration under winter lake ice cover (e.g., *42*). This is supported by water nutrient analyses that demonstrate Litla Viðarvatn has higher TOC/DOC than Stóra Viðarvatn in both summer and winter (*29*). Given that Stóra and Litla Viðarvatn are only separated by 0.6 km (Fig. 1B), any differences in *sed*aDNA and GDGT proxy records must therefore be controlled by non-climate factors, such as lake morphometry and/or physical-chemical properties.

Impact of oxygen availability on sedaDNA preservation

Our dual lake, multi-proxy approach reveals that Holocene oxygen availability differed substantially between the two lakes. In Stóra Viðarvatn, low isoGDGT-0/crenarchaeol values suggest the minimal presence of archaeal methanogens, except for possibly between 2900 and 1000 BP (Fig. 5A), implying that the water column and/or sediment oxygen concentrations remained at relatively high levels throughout the Holocene. In contrast, isoGDGT-0/crenarchaeol ratios in Litla Viðarvatn are elevated from 8000 BP through today (Fig. 5B), suggesting that water column and/or sediment oxygen concentrations have been consistently low, at least seasonally. As brGDGT concentrations have been shown to increase under anoxic conditions in some cases (e.g., *25*), the increase in Litla Viðarvatn brGDGT concentrations alongside increased isoGDGT-0/crenarchaeol at 8000 BP (Fig. 5D) may further support this state shift towards low oxygen conditions. However, a similar magnitude of brGDGT concentrations is found in Stóra Viðarvatn (Fig. 5C) despite GDGT-0/crenarchaeol ratios indicating a relatively oxic lake system, and that long-term trends in the two proxies are decoupled. This suggests that brGDGT concentrations may not always be influenced by oxygen availability.

*Sed*aDNA quality metrics indicate that DNA is poorly preserved in Litla Viðarvatn prior to 8000 BP (Fig. S4). Failure to identify plant *sed*aDNA in Litla Viðarvatn at this time is likely due to a lack of *trnL* amplification targets rather than inhibition given the uniformity of cycle threshold (C_T) values throughout the core. Based on the same timing of oxygen availability inferred from isoGDGT-0/crenarchaeol, we therefore infer that the more oxic lake environment accelerated DNA degradation in Litla Viðarvatn’s earliest record. This is supported by bulk geochemistry that shows this sediment is predominately aquatic in origin

and has low TOC (Fig. 4), which is consistent with the susceptibility of aquatic carbon in lakes to oxic remineralization (*43*). Shallow Arctic lakes like Litla Viðarvatn are sensitive to both UV radiation due to low DOC and long summer days (*44*) and temperature change due to their small volume (Fig. 2B). A sediment record from a small lake on Svalbard highlights that the impact of UV radiation was even stronger during the Early Holocene when UV-attenuating compounds, such as DOC, were even more limited due to the preceding glaciation (*45*). Given that experimental studies indicate that oxygen, UV radiation, and temperature can all influence DNA preservation (*24, 46-48*), UV radiation and higher summer temperatures likely compounded oxic DNA degradation in Litla Viðarvatn during the Early Holocene.

In contrast to Litla Viðarvatn, Stóra Viðarvatn‘s Holocene *sed*aDNA record is well preserved (*30*), despite that the lake has been oxic thoughout the Holocene (Fig. 5a). A survey of modern high-latitude lake surface sediments indicates that deep lakes generally promote DNA preservation (*49*). Stóra Viðarvatn‘s *sed*aDNA preservation may therefore be elevated by greater water depths that shield the sediment from UV radiation as well as lower seasonal temperatures (Fig. 2A). This suggests that the interplay of environmental variables that accelerate DNA degradation is complex and that identifying lakes that will yield valuable *sed*aDNA records may counter prevailing practices. For example, even though small high-latitude lakes are often targeted for *sed*aDNA studies (e.g., *38*), deeper lakes may be more suitable for such pursuits (*49*). In addition, sediment cores retrieved from below an oxycline (i.e., anoxic) in any sized lake will likely yield well-preserved *sed*aDNA records. As the pattern of postglacial plant colonization is one current focus in *sed*aDNA research (*13, 30, 50, 51*), our results highlight that reducing conditions and oxygen availability in lakes is an important consideration, and that shallow and/or intermittently oxic lakes like Litla Viðarvatn may not reliably preserve the *sed*aDNA needed to address this fundamental question.

Impact of oxygen and climate on brGDGT-based temperature records

Our comparison of brGDGTs in two different lakes demonstrates how oxygen availability may impact the reliability of brGDGT-based temperature reconstructions. The similarity between brGDGT distributions in Stóra and Litla Viðarvatn compared to modern Icelandic lake sediments (*16*) suggests at least partial *in situ* brGDGT production in both lakes (Fig. S3). However, Litla Viðarvatn and Icelandic soils share higher fractional abundances of pentamethylated brGDGTs (Fig. S3A) (*52*). Along with Litla Viðarvatn’s relatively low brGDGT ΣIIIa/ΣIIa ratios (0.59 and 0.92, Fig. S3E), some of the Litla Viðarvatn‘s brGDGTs may also be derived from catchment soils (*53, 54*) and/or modified by oxygen availability (*55*). Low oxygen conditions are known to alter lake sediment brGDGT distributions (*56, 57*), possibly by shifting production to methanotrophs in colder bottom waters and altering microbial community composition (*25*). Given the evidence for low oxygen availability in Litla Viðarvatn after 8000 BP (high isoGDGT/crenarchaeol), we assume that brGDGTs for most of the record reflect some combination of temperature and changes in microbial community composition, and therefore unreliable as a paleotemperature record.

The difference between Stóra Viðarvatn‘s brGDGT distributions and Icelandic soils provides confidence that *in situ* aquatic brGDGT production has dominated the sediment pool and that the application of lake specific brGDGT temperature calibrations is appropriate. Moreover, low isoGDGT/crenarchaeol ratios indicate that oxygen has not likely altered brGDGT sources (Fig. 5A). The qualitative MBT'_{5Me} index, which has been widely used in various brGDGT lake temperature calibrations (e.g., *58-59*), yields a relatively flat record for Stóra Viðarvatn (Fig. 5E), similar to Skorarvatn, a lake in northwest

Iceland (*36*). While the insensitivity of the MBT'$_{5Me}$ to temperature in Icelandic lake sediments is currently unclear, a recent lake brGDGT mesocosm study shows a limited sensitivity of MBT'$_{5Me}$ to low ambient temperatures (*60*). Similarly, we find that global and Arctic months above freezing (MAF) lake temperature calibrations, which use a multilinear regression model (*16-17*), also produce relatively flat records for Stóra Viðarvatn (Fig. 5G). In contrast to indices such as mean summer temperature (MST), MAF is challenging to interpret as a short, warm season may have the same value as a relatively long, mild season. In addition to the fact that MST is a more important control on high-latitude plant communities (e.g., *4*), we do not currently use the MAF metric.

Using an Icelandic lake brGDGT temperature calibration that relies on the strong relationship between the unsaturation of haptophyte alkenones and summer temperature (*36*), MST anomalies for Stóra Viðarvatn reveal a pattern consistent with qualitative and quantitative lake temperature histories in Iceland (*12, 36*). More specifically, we find the highest MST anomalies during the Early Holocene (+1.75 ºC, Fig. 5I) followed by general summer cooling during the Middle and Late Holocene to the lowest MST anomalies (-2.0 ºC, Fig. 5I). If temperatures from Litla Viðarvatn are considered prior to the onset of long-term oxygen limitation, peak Early Holocene temperatures for this region of Iceland were up to 2.1 ºC higher than today (Fig. 5J). While oxygen availability does not generally affect Stóra Viðarvatn, elevated isoGDGT-0/crenarchaeol ratios between 2900 and 1000 BP suggest a possible period of low oxygen conditions, making this interval questionable for temperature interpretation. In contrast to Litla Viðarvatn, where persistent changes in oxygen have likely confounded the brGDGT climate record over the last 8000 years, the brGDGT record from Stóra Viðarvatn highlights that lake sediment records from oxic locations can yield higher quality records of temperature variability. As commonly targeted shallow lakes are often stratified and seasonally anoxic in the Arctic (*26*), we recommend using lake sediments acquired from above the seasonal oxycline or an oxic lake like Stóra Viðarvatn for the optimal use of brGDGTs in paleotemperature reconstructions.

Climate driven changes in Holocene plant assemblages

Our dual lake approach circumvents the impact of oxygen availability on brGDGT and *sed*aDNA proxies and demonstrates that regional climate has been the primary forcing behind Holocene vegetation change in Iceland. Total species richness in Stóra and Litla Viðarvatn increases through the Holocene with a substantial increase at ~4000 BP in both lakes (Fig. 6). The increase in plant species richness at 4000 BP corresponds with a transition from woodland to heathland environment, marked by the consistent presence of *Vaccinium* and *Carex*, as well as cold- (e.g., *Bistorta* and *Oreojuncus*) and dry-tolerant taxa (e.g., *Galium, Ranunculus,* and *Saxifraga*) (Fig. 6). Our independent MST anomaly estimates from Stóra Viðarvatn are inversely related to species richness in both lakes, recording peak summer temperature anomalies during the Early Holocene (+1.75 ºC and +2.1 ºC in Litla Viðarvatn) when species richness is low and lower summer temperature anomalies (-2.0 ºC) during the Late Holocene when species richness is high (Fig. 7A-B). Outside of Iceland, *sed*aDNA studies from Holocene lakes in northern Fennoscandia (*38*) and Late Quaternary sites across the Arctic (*11*) also show relatively increased plant species richness during the Late Holocene (4200 BP to present) and Last Glacial Maximum (26,500 to 19,000 BP), two periods that were broadly colder than today. The broad consistency across these Arctic and sub-Arctic sites demonstrates that summer temperature has been at least one control on Holocene plant community patterns in the high latitudes, including Iceland.

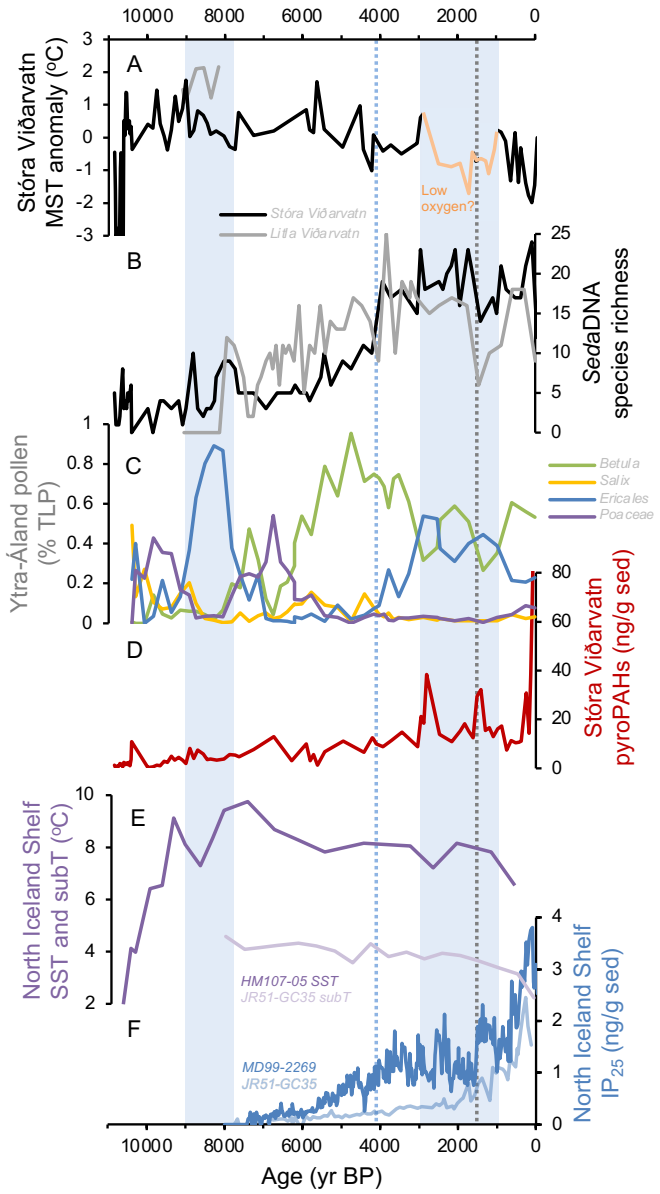

Fig. 7. Regional climate record comparisons. (**A**) Stóra and Litla Viðarvatn MST anomalies (ºC, this study) where orange portion between 2900 and 1000 BP reflects a potential influence of suboxic conditions, (**B**) Stóra and Litla Viðarvatn *sed*aDNA species richness (this study), (**C**) Ytra-Áland pollen (%TLP, total land pollen (*62*)), (**D**) Stóra Viðarvatn pyroPAHs (ng/g sed (*14*)), (**E**) eastern North Iceland Shelf sea surface (HM107-05, (*66*)) and subsurface temperatures (JR51-GC35 (*65*)), and (**F**) North Iceland Shelf sea ice records based on the IP_{25} biomarker (ng/g sed) from sites MD99-2269 and JR51-GC35 (*64*). Vertical blue bars highlight peaks in Ericales and heathland inferred from Ytra-Áland pollen. Dashed blue line at 4000 BP marks the onset of local heathland expansion and dashed gray line at 1500 BP indicates the onset of local soil erosion.

A Holocene pollen record from Ytra-Áland, a peat section located ~12 km east of Stóra and Litla Viðarvatn (Fig. 1A), provides complementary information on changes in past plant communities as, unlike DNA, pollen generally reflects taxa abundance (*61*). From 9000 to 7900 BP and from 2900 to 1000 BP, the relative abundance of *Betula* pollen (green, Fig. 7C) decreases at the expense of Ericales (blue, Fig. 7c), reflecting periods of local

heathland environments (*62*). Prior to 2900 BP, Ericales pollen begins to increase at 4000 BP (Fig. 7C), which is consistent with additional local peat pollen records reflecting the Late Holocene expansion of heathland (*63*), the timing of increased *sed*aDNA species richness (Fig. 7B), declining MST anomalies (Fig. 7A), and increased sea ice presence on the North Iceland Shelf (Fig. 7F) (*64*). Between 2900 and 1000 BP, increased fire frequency reconstructed from pryogenic polycyclic aromatic hydrocarbons (pyroPAHs) in Stóra Viðarvatn (Fig. 7D) (*14*) further suggests a relatively dryer, cooling climate that may have preconditioned the environment to natural forest fires at this time. Broadly, these climate changes follow a regional pattern of Late Holocene cooling observed in eastern North Iceland Shelf surface and subsurface temperatures (*65, 66*) and drift ice (*64*).

While the plant *sed*aDNA records from Stóra and Litla Viðarvatn show broadly similar patterns, one key difference between the two is the diversity of aquatic taxa. Bulk geochemical proxies (high $\delta^{13}C$ and low C/N) indicate that organic matter in Litla Viðarvatn is predominately aquatic (Fig. 5F and H) (*12*), which is consistent with higher diversity of aquatic taxa DNA (Fig. 6) and with the shallowness of the lake that permits light penetration needed for higher photosynthetic rates. Litla Viðarvatn‘s record includes two notable aquatic taxa that inhabit clear and calm waters: *Isoetes* and *Callitriche*. Whereas some cosmopolitan aquatic taxa (e.g., Potamogetonaceae and *Myriophyllum*) are present throughout the record, *Isoetes* and *Callitriche* dissappear after 1450 and 2150 BP, respectively (Fig. 6). Based on bulk geochemistry records from Stóra and Litla Viðarvatn ($\delta^{13}C$ and C/N), the onset of persistent Late Holocene soil erosion begins at 1500 BP (Fig. 5) (*14*), which likely enhanced water turbiditiy and limited *Isoetes* production. A sharp decrease in Litla Viðarvatn‘s BSi occurs at 1500 BP as well (Fig. 5D and J), suggesting diatom productivity may have also decreased possibly due to increased soil erosion and more limited sunlight transmission. Considering the current debate on the onset and origins of soil erosion in Iceland (i.e., natural vs anthropogenic) (12, 14), our bulk geochemistry and plant *sed*aDNA evidence argues for the onset prior to local human occupation (~1010 BP/940 CE) (*67*), and therefore a natural driver. The coincidental timing of increased soil erosion in northeast Iceland and drift ice on the North Iceland Shelf at 1500 BP suggests that the rapid expansion of Polar water masses around Iceland played an important role in these natural environmental changes (Fig. 7F).

The presence and environmental impact of humans in Icelandic lake sediments has largely been assumed based on the timing of acknowledged Norse settlement (~1080 BP), although some proxies diagnostic of human presence have been proposed (*12*). Of these proxies, fecal sterols (biomarkers produced in mammal intestinal tracts) and mammalian *sed*aDNA of humans and/or their domestic livestock offer the best promise as they are more direct indicators of human presence in the catchment (*21-23*). In Iceland, fecal biomarker records from Stóra Viðarvatn only show concentrations above background levels in recent centuries, suggesting that following Norse settlement there was either 1) no substantial mammalian population or 2) fecal sterols were diluted in a large lake (*14*). Even with Litla Viðarvatn‘s considerably smaller size and higher TOC content (i.e., less minerogenic dilution), our DNA metabarcoding and target capture efforts, which are more source-specific than fecal biomarkers, failed to yield reads for domestic livestock in either lake. Coupled with the positive identification of sheep DNA in our test validation site (Vestra Gílsholtsvatn), the null results from Stóra and Litla Viðarvatn indicate that the lack of mammalian *sed*aDNA reads is likely due to low sheep populations (e.g., *22*). As we also observe no substantial changes in bulk geochemistry or *sed*aDNA environmental proxies following local human settlement at ~1010 BP/870 CE, we infer that humans and their livestock have left a limited footprint on the local terrestrial environment (e.g., *14*). As other Icelandic *sed*aDNA records report ecosystem disturbances following settlement (e.g., *13*),

our records indicate predominately climate-driven Holocene environmental change and therefore robust empirical constraint for climate and vegetation models.

In conclusion, to provide robust constraints for predictive models, reconstructing past climate-plant dynamics requires quality records of local climate and plant assemblage. However, two of the most promising proxy methods in the field (brGDGTs and plant *sed*aDNA) often require contrasting lake mixing regimes for reliable paleoenvironmental interpretations. Our results from Iceland demonstrate that brGDGTs are best applied in oxic lakes whereas plant *sed*aDNA is best preserved in stratified, low oxygen settings, highlighting that both climate and plant history can be challenging to reconstruct from one site alone. This may be one reason why their analysis from the same sediment records is rare (e.g., *50*). As shallow lakes may also capture relatively greater proportions of aquatic plant DNA compared to deeper lakes (*20*), applying a dual lake approach, with geographically proximal oxic and low oxygen lakes, can overcome these hurdles and lead to more holistic and detailed records of climate-plant dynamics in sites across the high latitudes.

Materials and Methods

Modern water quality and water chemistry

Stóra Viðarvatn (66.24°N, 15.84°W) is a relatively large (2.5 km^2), deep lake (48 m), and Litla Viðarvatn (66.24°N, 15.81°W) is a relatively small (0.2 km^2), shallow lake (2.5 m) – both located at located at 151 m asl and separated by 0.6 km in NE Iceland (Fig. 1). We used iButtons loggers (Thermochron DS1925L, Maxim Integrated Products) to measure *in situ* surface and bottom water (20 m depth) temperatures in Stóra Viðarvatn and surface water temperature only in Litla Viðarvatn (due to the shallow water depth) at 6-hour intervals between September 2019 and September 2020 (Fig. 2A-B) (*68*). We also measured temperature, pH, dissolved oxygen, and conductivity with a multiparameter probe (HydroLab HL4, OTT HydroMet) at ~0.5-m increments along vertical profiles at each lake's coring location in September 2019 and February 2020 (Fig. 2C-D and S1) (*29*). We note that bottom water measurements taken for Stóra Viðarvatn are not from the deepest portion of the lake (48 m depth), which is located south of the sampling site (20 m depth) Fig. 1B).

Lake sediment cores and chronology

In February 2020, we recovered an 8.93 m long core from Stóra Viðarvatn (20SVID-02) and a 7.25 m long core from Litla Viðarvatn (20LVID-02/01) atop lake ice platforms using Bolivia coring systems (Fig. 1B). 20SVID-02 was collected in 7 continuous drives, whereas 20LVID-02/01 was collected in 2 overlapping drives. Sediment sections were photographed and measured for magnetic susceptibility (MS) at the University of Minnesota's Continental Scientific Drilling Facility, the latter of which was used to splice sections 20LVID-02 and 20LVID-01 into a single composite sediment record (Fig. S2). Core sections were stored at 4 ºC until sampling was conducted for proxy analyses.

Bayesian age models for Stóra Viðarvatn have been previously published, which use 13 visible tephra layers of known age and their geochemical fingerprints (*14, 30*). For Litla Viðarvatn, age control is based on 11 radiocarbon ages from moss macrofossils (Table S1) and 2 marker tephra layers identified visually (G10ka Series, 10400 to 9900 BP (*31*) and Hekla 3, 3010 ± 54 BP (*32*)). Radiocarbon samples were given an acid-base-acid pretreatment and graphitized at the University of Colorado Boulder, then measured by AMS at the University of California Irvine. The two marker tephra sequences/layers identified in Litla Viðarvatn are widely dispersed across Iceland (*31, 69*), form relatively thick, coarse-grained local deposits (Fig. S2), and are geochemically confirmed in the sediment record

from Stóra Viðarvatn (*14, 30*). We generated a Bayesian age model for Litla Viðarvatn using the R package rbacon, default model functions (*70*), and the IntCal20 calibration curve (*71*). For the 9-cm-thick Hekla 3 tephra layer, we used the 'slump' function in rbacon to represent its instantaneous deposition (Fig. 3). For the G10ka Series, we only used the upper boundary dated to ~9900 BP as the Litla Viðarvatn sediment record's bottom ends within the tephra unit and it is unclear if the entire tephra unit extending back to ~10400 BP was recovered.

Bulk sediment geochemistry

Stóra Viðarvatn's bulk geochemical record has been previously published and is based on 181 samples (*14*). 150 new samples were taken from Litla Viðarvatn and measured for total carbon (TC), total nitrogen (TN), and $\delta^{13}C$ (relative to VPDB) on a PDZ Europa ANCA-GSL elemental analyzer interfaced to a PDZ Europa 20-20 isotope ratio mass spectrometer at the University of California Davis Stable Isotope Facility. We did not decalcify the samples from either lake sediment record due to the limited stock of inorganic carbon in and around the lakes, and therefore take TC to reflect total organic carbon (TOC) (*14*). For each of these samples, we also measured biogenic silica by diffuse reflectance Fourier Transform Infrared Spectrometry (FTIRS) on a Bruker Vertex 70 with a Praying Mantis diffuse reflectivity accessory (Harrick) at the University of Colorado Boulder. We report values in FTIRS absorbance units.

Lipid biomarkers

At the University of Colorado Boulder Organic Geochemistry Laboratory, we freeze-dried 54 sediment samples from Litla Viðarvatn (~1–2 g) and extracted each two times on a Dionex accelerated solvent extractor (ASE 350) using dichloromethane (DCM):methanol (9:1, v/v) at 100 °C and 1500 psi. For Stóra Viðarvatn, we used 83 previously extracted samples (*14*). A 5 or 10 % aliquot of total lipid extracts (TLE) were taken for glycerol dialkyl glycerol tetraether (GDGT) analysis, resuspended in *n*-hexane:isopropanol (99:1, v/v), sonicated, vortexed, and then filtered using a 0.45 μm polytetrafluoroethylene (PTFE) syringe filter. Prior to analysis, samples were spiked with 10 ng of the C_{46} GDGT internal standard (*72*). GDGTs were identified and quantified via high-performance liquid chromatography–mass spectrometry (HPLC-MS) following modified methods of Hopmans et al. (*ref 73*) on a Thermo Scientific Ultimate 3000 HPLC interfaced to a Q Exactive Focus Quadrupole-Orbitrap MS (*16*). Isoprenoid and branched GDGTs were identified based on their characteristic masses and elution patterns.

To reconstruct past environmental conditions, we used a variety of published indices and temperature calibrations that rely on the distribution and fractional abundance of isoprenoid and branched GDGTs. While many regional and global temperature calibrations exist for lake sediment brGDGTs, we focus on those that are either local to Iceland (*36*) or "global" and incorporate Icelandic lake sediment samples (*16, 17*). This rationale is supported by recent statistical analyses that demonstrate regional clustering of global brGDGT distributions and advocate for site-specific or regional calibrations (*74*).

First, we used the ratio of isoGDGT-0/crenarchaeol as a proxy for the presence of archaeal methanogens (*27*). For relative temperature, we used the MBT'_{5ME} (*35*), which while not including samples from Iceland, forms the basis of many lake brGDGT calibrations:

$$MBT'_{5ME} = ([Ia] + [Ib] + [Ic])/([Ia] + [Ib] + [Ic] + [IIa] + [IIb] + [IIc] + [IIIa])$$

For quantitative temperature estimates, we used an *in-situ* lake brGDGT calibration from Skorarvatn (*36*), a lake in NW Iceland (Fig. 1a), that capitalizes on the strong relationship

between the unsaturation of alkenones, a separate class of lipids produced by haptophyte algae, and summer temperature (U^{K}_{37}) (*75*):

$$U^{K}_{37} = -0.1540 \times [IIIa] + 0.3538 \times [Ia] + 1.0016 \times [IIIa'] - 0.7537$$
$$U^{K}_{37} = 0.0287 \times T$$

While this calibration was developed for Skorarvatn's sediment record specifically, we argue that the application for at least Stóra Viðarvatn is reasonable given the similar water depths of core sites (25 vs 20 m depth, respectively), and therefore, likely similar seasonal water properties. In addition, we used three global lake temperature calibrations that incorporate high latitude and highly seasonal regions, including Iceland, and reconstruct temperature using the months above freezing (MAF) metric (*16, 17*). The first is based on the traditional calculation of brGDGT fractional abundance against all 15 major brGDGTs (i.e., Full Set) (*16*):

$$MAF = -8.06 + 37.52 \times [fIa] - 266.83 \times [fIb]^2 + 133.42 \times [fIb] + 100.85 \times [fIIa']^2 + 58.15 \times [fIIIa']^2 + 12.79 \times [fIIIa]$$

The second is based on a revised fractional abundance calculation that isolates structural groups, such as methylation number and position and cyclization number (i.e., Methylation Set) (*16*):

$$MAF = 92.9 + 63.84 \times [fIb_{Meth}]^2 - 130.51 \times [fIb_{Meth}] - 28.77 \times [fIIa_{Meth}]^2 - 72.28 \times [fIIb_{Meth}]^2 - 5.88 \times [fIIc_{Meth}]^2 + 20.89 \times [fIIIa_{Meth}]^2 - 40.54 \times [fIIIa_{Meth}] - 80.47 \times [fIIIb_{Meth}]$$

Finally, we used an Arctic lakes temperature calibration that uses the traditional calculation of brGDGT fractional abundance against all 15 major brGDGTs (i.e., Full Set) and the months above freezing (MAF) metric (*17*):

$$MAF = 17.0 - 11.4 \times [fIIa] - 17.4 \times [fIIIa] - 15.9 \times [fIIa'] - 124.4 \times [fIIIb]$$

DNA metabarcoding

All DNA sampling was conducted in a dedicated clean lab facility with no PCR products in the University of Colorado Boulder Trace Metal Lab. Stóra Viðarvatn's *sed*aDNA plant DNA record has been previously published and is based on 75 samples (*30*). For Litla Viðarvatn, we took 54 samples immediately after splitting the sediment cores. Biomarker samples, as described above, were collected from the same intervals as DNA samples, ensuring that the two timeseries are time locked.

We performed sample extraction and processing in a dedicated ancient DNA laboratory at the University of California Santa Cruz Paleogenomics Lab. Before sample extraction, we compared three sedimentary DNA extraction methods (*76-78*) to evaluate their individual performance for Icelandic lake sediment (see Supplementary Materials). Based on these results, we extracted lake sediment samples following Rohland et al. (*ref 76*). Complete methods for extraction, quantitative PCR (qPCR), *trnL* metabarcoding, sequencing, and bioinformatic processing are provided in the Supplementary Materials and are identical to those previously published for Stóra Viðarvatn (*30*).

For mammalian DNA, we tested several metabarcoding primers and methods. We initially generated metabarcoding libraries for 16Smamm (*40*) on the extraction comparison sample set as well as two sheep specific targeting primer sets (*41*), and then focused efforts on the shorter mammP007 primer in tandem with previously described human blocking

oligos (*22*). The sheep specific and mammP007 primers were tested on a subset of lake sediment samples from Stóra and Litla Viðarvatn. Complete methods for sequencing and bioinformatic processing are provided in the Supplementary Materials. Lastly, we generated single stranded shotgun libraries from a subset of Litla Viðarvatn lake sediment samples using the Santa Cruz library preparation method (*79*) and performed hybridization capture with a mammalian mitochondrial genome targeting Arbor mybaits set (*80*) and modified to include additional taxa (see Supplementary Materials). To validate the mammalian DNA tests, we collected and analyzed two modern soil and lake surface sediment samples from south Iceland where sheep are prevalent today (Vestra Gíslholtsvatn, Fig. 1A).

References

1. I.H. Myers-Smith, B.C. Forbes, M. Wilmking, M. Hallinger, T. Lantz, D. Blok, K.D. Tape, M. Macias-Fauria, U. Sass-Klaassen, E. Lévesque, S. Boudreau, P. Ropars, L. Hermanutz, A. Trant, L.S. Collier, S. Weijers, J. Rozema, S.A. Rayback, N.M. Schmidt, G. Schaepman-Strub, S. Wipf, C. Rixen, C.B. Ménard, S. Venn, S. Goetz, L. Andreu-Hayles, S. Elmendorf, V. Ravalainen, J. Welker, P. Groan, H.E. Epstein, D.S. Hik, Shrub expansion in tundra ecosystems: dynamics, impacts and research priorities. *Environ. Res. Lett.* **6**, 045509 (2011).
2. R.J. Dial, C.T. Maher, R.E. Hewitt, A.M. Wockenfuss, R.E. Wong, D.J. Crawford, M.G. Zietlow, P.F. Sullivan, Arctic sea ice retreat fuels boreal forest advance. *Science* **383**, 877-884 (2024).
3. K. Tape, M. Sturm, C. Racine, The evidence for shrub expansion in Northern Alaska and the Pan-Arctic. *Glob. Change Biol.* **12**, 686–702 (2006).
4. S.C. Elmendorf, G.H.R. Henry, R.D. Hollister, R.G. Björck, N. Boulanger-Lapointe, E.J. Cooper, J.H.C. Cornelissen, T.A. Day, E. Dorrepaal, T.G. Elumeeva, M. Gill, W.A. Gould, J. Harte, D.S. Hik, A. Hofgaard, D.R. Johnson, J.F. Johnstone, I.S. Jónsdóttir, J.C. Jorgensen, K. Klanderud, J.A. Klein, S. Koh, G. Kudo, M. Lara, E. Lévesque, B. Magnússon, J.L. May, J.A. Mercado-Díaz, A. Michelsen, U. Molau, I.S. Myers-Smith, S.F. Oberbauer, V.G. Onipchenko, C. Rixen, N.M. Schmidt, G.R. Shaver, M.J. Spasojevic, Þ.E. Þórhallsdóttir, A. Tolvanen, T. Troxler, C.E. Tweedie, S. Villareal, C.-H. Wahren, X. Walker, P.J. Webber, J.M. Welker, S. Wipf, Plot-scale evidence of tundra vegetation change and links to recent summer warming. *Nat. Clim. Change* **2**, 453-457 (2012).
5. M. Sturm, T. Douglas, C. Racine, G.E. Liston, Changing snow and shrub conditions affect albedo with global implications. *J. Geophys. Res.* **110**, 1–13 (2005).
6. R.G. Pearson, S.J. Phillips, M.M. Loranty, P.S.A. Beck, T. Damoulas, S.J. Knight, S.J. Goetz, Shifts in Arctic vegetation and associated feedbacks under climate change. *Nat. Clim. Change* **3**, 673–677 (2013).
7. A.J. Thompson, J. Zhu, C.J. Poulsen, J.E. Tierney, C.B. Skinner, Northern Hemisphere vegetation change drives a Holocene thermal maximum. *Sci. Adv.* **8**, eabj6535 (2022).
8. P. Fauchald, T. Park, H. Tømmervik, R. Myneni, V.H. Hausner, Arctic greening from warming promotes declines in caribou populations. *Sci. Adv.* **3**, e1601365 (2017).
9. C.G. Collins, J.E. Stajich, S.E. Weber, N. Pombubpa, J.M. Diez, Shrub range expansion alters diversity and distribution of soil fungal communities across an alpine elevation gradient. *Mol. Ecol.* **27**, 2461–2476 (2018).
10. S.E. Crump, B. Fréchette, M. Power, S. Cutler, G. de Wet, M.K. Raynolds, J.H. Raberg, J.P. Briner, E.K. Thomas, J. Sepúlveda, B. Shapiro, M. Bunce, G.H. Miller, Ancient plant DNA reveals High Arctic greening during the last interglacial. *Proc. Natl. Acad. Sci.* **118**, 1–9 (2021).
11. Y. Wang, M.W. Pedersen, I.G. Alsos, B. De Sanctis, F. Racimo, A. Prohaska, E. Coissac, H.L. Owens, M.K.F. Merkel, A. Fernandez-Guerra, A. Rouillard, Y. Lammers, A. Alberti, F.

Denoeud, D. Money, A.H. Ruter, H. McColl, N.K. Larsen, A.A. Cherezova, M.E. Edwards, G.B. Federov, J. Haile, L. Orlando, L. Vinner, T.S. Korneliussen, D.W. Beilman, A.A. Bjørck, J. Cao, C. Dockter, J. Esdale, G. Gusarova, K.K. Kjeldsen, J. Mangerud, J.T. Rasic, B. Skadhauge, J.I. Svendsen, A. Tikhonov, P. Wincker, Y. Xing, Y. Zhang, D.G. Froese, C. Rahbek, D.B. Nogues, P.B. Holden, N.R. Edwards, R. Durbin, D.J. Meltzer, K.H. Kjær, P. Möller, E. Willerslev, Late Quaternary dynamics of Arctic biota from ancient environmental genomics. *Science* **600**, 86-92 (2021).

12. Á. Geirsdóttir, D.J. Harning, G.H. Miller, J.T. Andrews, Y. Zhong, C. Caseldine, Holocene history of landscape instability in Iceland: Can we deconvolve the impacts of climate, volcanism and human activity? *Quat. Sci. Rev.* **249**, 106633 (2020).
13. I.G. Alsos, Y. Lammers, S.E. Kjellman, M.K.F. Merkel, E.M. Bender, A. Rouillard, E. Erlendsson, E.R. Guðmundsdóttir, I.Ö. Benediktsson, W.R. Farnsworth, S. Brynjólfsson, G. Gísladóttir, S.D. Eddudóttir, A. Schomacker, Ancient sedimentary DNA shows rapid post-glacial colonisation of Iceland followed by relatively stable vegetation until the Norse settlement (Landnám) AD 870. *Quat. Sci. Rev.* **259**, 106903 (2021).
14. N. Ardenghi, D.J. Harning, J.H. Raberg, B.R. Holman, T. Thordarson, Á. Geirsdóttir, G.H. Miller, J. Sepúlveda, A Holocene history of climate, fire, landscape evolution, and human activity in Northeast Iceland. *Clim. Past* **20**, 1087-1123 (2024).
15. D.J. Harning, C.R. Florian, Á. Geirsdóttir, T. Thordarson, G.H. Miller, Y. Axford, S. Ólafsdóttir, High-resolution Holocene record based on detailed tephrochronology from Torfdalsvatn, north Iceland, reveals natural and anthropogenic impacts on terrestrial and aquatic environments. *Clim. Past*, *in revision* (2024).
16. J.H. Raberg, D.J. Harning, S.E. Crump, G. De Wet, A. Blumm, S. Kopf, Á. Geirsdóttir, G.H. Miller, J. Sepúlveda, Revised fractional abundances and warm-season temperatures substantially improve brGDGT calibrations in lake sediments. *Biogeosciences* **18**, 3579–3603 (2021).
17. G.A. Otiniano, T.J. Porter, M.A. Phillips, S. Juutinen, J.B. Weckström, M.P. Heikkilä, Reconstructing warm-season temperatures using brGDGTs and assessing biases in Holocene temperature records in northern Fennoscandia. *Quat. Sci. Rev.* **329**, 105555 (2024).
18. P. Sjögren, M.E. Edwards, L. Gielly, C.T. Langdon, I.W. Croudace, M.K.F. Merkel, T. Fonville, I.G. Alsos, Lake sedimentary DNA accurately records 20th Century introductions of exotic conifers in Scotland. *New Phytol.* **213**, 929–941 (2017).
19. I.G. Alsos, Y. Lammers, N.G. Yoccoz, T. Jørgensen, P. Sjögren, L. Gielly, M.E. Edwards, Plant DNA metabarcoding of lake sediments: how does it represent the contemporary vegetation. *PLOS ONE* **13**, e0195403 (2018).
20. E. Capo, C. Giguet-Covex, A. Rouillard, K. Nota, P.D. Heintzman, A. Vuillemin, D. Ariztegui, F. Arnaud, S. Belle, S. Bertilsson, C. Bigler, R. Bindler, A.G. Brown, C.L. Clarke, S.E. Crump, D. Debroas, G. Englund, G.F. Ficetola, R.E. Garner, J. Gauthier, I. Gregory-Eaves, L. Heinecke, U. Herzschuh, A. Ibrahim, V. Kisand, K.H. Kjær, Y. Lammers, J. Littlefair, E. Messager, M.-E. Monchamp, F. Olajos, W. Orsi, M.W. Pedersen, D.P. Rijal, J. Rydberg, T. Spanbauer, K.R. Stoof-Leichsenring, P. Taberlet, L. Talas, C. Thomas, D.A. Walsh, Y. Wang, E. Willerslev, A. van Woerkom, H.H. Zimmermann, M.J.L. Coolen, L.S. Epp, I. Domaizon, I.G. Alsos, L. Parducci, Lake sedimentary DNA research on past terrestrial and aquatic biodiversity: overview and recommendations. *Quaternary* **4**, 6 (2021).
21. L. Curtin, W.J. D'Andrea, N.L. Balascio, S. Shirazi, B. Shapiro, G.A. de Wet, R.S. Bradley, J. Bakke, Sedimentary DNA and molecular evidence for early human occupation of the Faroe Islands. *Commun. Earth Environ.* **2**, 253 (2021).
22. C., Giguet-Covex, J. Pansu, F. Arnaud, P.J. Rey, C. Griggo, L. Gielly, I. Domaizon, E. Coissac, F. David, P. Choler, J. Poulenard, P. Taberlet, Long livestock farming history and human landscape shaping revealed by lake sediment DNA. *Nat. Comm.* **5**, 3211 (2014).

23. S. Garcés-Pastor, E. Coissac, S. Lavergne, C. Schwörer, J.-P. Theurillat, P.D. Heintzman, O.S. Wangensteen, W. Tinner, F. Rey, M. Heer, A. Rutzer, K. Walsh, Y. Lammers, A.G. Brown, T. Goslar, D.P. Rijal, D.N. Karger, L. Pellissier, The PhyloAlps Consortium, O. Heiri, I.G. Alsos, High resolution ancient sedimentary DNA shows that alpine plant diversity is associated with human land use and climate change. *Nat. Comm.* **13**, 6559 (2022).
24. T. Lindahl, Instability and decay of the primary structure of DNA. *Nature* **362**, 709– 715 (1993).
25. Y. Weber, J.S. Sinninghe Damste, J. Zopfi, C. De Jonge, A. Gilli, C.J. Schubert, F. Lepori, M.F. Lehmann, H. Niemann, Redox-dependent niche differentiation provides evidence for multiple bacterial sources of glycerol tetraether lipids in lakes. *Proc. Natl. Acad. Sci.* **115**, 10926–10931 (2018).
26. Y. Klanten, R.-M. Couture, K.S. Christoffersen, W.F. Vincent, D. Antoniades, Oxygen depletion in Arctic lakes: Circumpolar trends, biogeochemical processes, and implications of climate change. *Global Biogeochemical Cycles* **37**, e2002GB007616 (2023).
27. C.I. Blaga, G.-J. Reichart, O. Heiri, J.S. Sinninghe Damsté, Tetraether membrane lipid distribution in water-column particulate matter and sediments: A study from 47 European lakes along a north-south transect. *J. Paleolimnol.* **41**, 535–540 (2009).
28. T. Schneider, I.S. Castañeda, B. Zhao, S. Krüger, J.M. Salacup, R.S. Bradley, Tracing Holocene temperatures and human impact in a Greenlandic Lake: Novel insights from hyperspectral imaging and lipid biomarkers. *Quat. Sci. Rev.* **339**, 108851, 2024.
29. J. Raberg, D. Harning, Á. Geirsdóttir, J. Sepúlveda, G.H. Miller, Water chemistry profiles of lakes in Iceland (2019-2021). Arctic Data Center [data set], http://doi.org/10.18739/A26688K7F (2023).
30. D.J. Harning, S. Sacco, K. Anamthawat-Jónsson, N. Ardenghi, T. Thordarson, J.H. Raberg, J. Sepúlveda, Á. Geirsdóttir, B. Shapiro, G.H. Miller, Delayed postglacial colonization of *Betula* in Iceland and the circum North Atlantic. *eLife* **12**, RP87749 (2023).
31. B.A. Óladóttir, T. Thordarson, Á. Geirsdóttir, G.E. Jóhannsdóttir, J. Mangerud, The Saksunarvatn Ash and the G10ka series tephra. Review and current state of knowledge. *Quat. Geochronol.* **56**, 101041 (2020).
32. A.J. Dugmore, G.T. Cook, J.S. Shore, A.J. Newton, K.L. Edwards, G. Larsen, Radiocarbon dating tephra layers in Britain and Iceland. *Radiocarbon* **37**, 379-388 (1995).
33. D.J. Conley, C.L. Schelske, Biogenic silica, in: Tracking environmental change using lake sediments, edited by: W.M. Last and J.P. Smol, Springer Science & Business Media, 281–293, ISBN 1402006284, 2002.
34. S. Naeher, F. Peterse, R.H. Smittenberg, H. Niemann, P.K. Zigah, C.J. Schubert, Sources of glycerol dialkyl glycerol tetraethers (GDGTs) in catchment soils, water column and sediments of Lake Rotsee (Switzerland)—Implications for the application of GDGT-based proxies for lakes. *Org. Geochem.* **66**, 164–173 (2014).
35. C. De Jonge, E.C. Hopmans, C.I. Zell, J.H. Kim, S. Schouten, J.S. Sinninghe Damsté, Occurrence and abundance of 6-methyl branched glycerol dialkyl glycerol tetraethers in soils: implications for palaeoclimate reconstruction. *Geochem. Cosmochim. Acta* **141**, 97-112 (2014).
36. D.J. Harning, L. Curtin, Á. Geirsdóttir, W.J. D'Andrea, G.H. Miller, J. Sepúlveda, Lipid biomarkers quantify Holocene summer temperature and ice cap sensitivity in Icelandic lakes. *Geophys. Res. Lett.* **47**, 1–11 (2020).
37. P. Taberlet, E. Coissac, F. Pompanon, L. Gielly, C. Miquel, A. Valentini, T. Vermat, G. Corthier, C. Brochmann, E. Willerslev, Power and limitations of the chloroplast *trnL* (UAA) intron for plant DNA barcoding. *Nucleic Acids Res.* **35**, e14 (2007).
38. D.P. Rijal, P.D. Heintzman, Y. Lammers, N.G. Yoccoz, K.E. Lorberau, I. Pitelkova, T. Goslar, M.J.A. Murguzur, J.S. Salonen, K.F. Helmens, J. Bakke, M.E. Edwards, T. Alm, K.A.

Bråthen, A.G. Brown, I.G. Alsos, Sedimentary ancient DNA shows terrestrial plant richness continuously increased over the Holocene in northern Fennoscandia. *Sci. Adv.* **7**, 1-16 (2021).
39. L.C. Ross, G. Austrheim, L.-J. Asheim, G. Bjarnason, J. Feilberg, A.M. Fosaa, A.J. Hester, Ø. Holand, I.S. Jónsdóttir, L.E. Mortensen, A. Mysterud, E. Olsen, A. Skonhoft, J.D.M. Speed, G. Steinheim, D.B.A. Thompson, A.G. Thórhallsdóttir, Sheep grazing in the North Atlantic region: A long-term perspective on environmental sustainability. *Ambio* **45**, 551-566 (2016).
40. P.G. Taylor, Reproducibility of ancient DNA sequences from extinct Pleistocene fauna. *Mol. Biol Evol.* **13**, 283–285 (1996).
41. D.W. Cai, L. Han, X.L. Zhang, H. Zhou, H. Zhu, DNA analysis of archaeological sheep remains from China. *J. Archaeol. Sci.* **34**, 1347–1355 (2007).
42. S. Golosov, O.A. Maher, E. Schipunova, A. Terzhevik, G. Zdorovennova, G. Kirillin, Physical background of the development of oxygen depletion in ice-covered lakes. *Oecologia* **151**, 331-430 (2007).
43. S. Sobek, E. Durisch-Kaiser, R. Zurbrügg, N. Wongfun, M. Wessels, N. Pasche, B. Wehrli, Organic carbon burial efficiency in lake sediments controlled by oxygen exposure time and sediment source. *Limnol. Oceanogr.* **54**, 2243-2254 (2009).
44. W.F. Vincent, R. Pienitz, Sensitivity of high-latitude freshwater ecosystems to global change: temperature and solar ultraviolet radiation. *Geoscience Canada* **23**, 231–236 (1996).
45. L. Nevalainen, M.V. Rantala, T.P. Luoto, M. Rautio, A.E.K. Ojala, Ultraviolet radiation exposure of a high arctic lake in Svalbard during the Holocene. *Boreas* **44**, 401-412 (2015).
46. T. Lindahl, B. Nyberg, Rate of depurination of native deoxyribonucleic acid. *Biochemistry* **11**, 3610– 3618 (1972).
47. K.M. Strickler, A.K. Fremier, C.S. Goldberg, Quantifying effects of UV-B, temperature, and pH on eDNA degradation in aquatic microcosms. *Biological Conservation* **183**, 85– 92 (2015).
48. H.S. Mejbel, W. Dodsworth, F.R. Rick, Effects of temperature and oxygen on cyanobacterial DNA preservation in sediments: A comparison study of major taxa. *Environ. DNA* **4**, 717-731 (2022).
49. W. Jia, X. Liu, K.R. Stoof-Leichsenring, S. Liu, K. Li, U. Herzschuh, Preservation of sedimentary plant DNA is related to lake water chemistry. *Environ. DNA* **4**, 425-439 (2021).
50. S.E. Crump, G.H. Miller, M. Power, J. Sepúlveda, N. Dildar, M. Coghlan, M. Bunce, Arctic shrub colonization lagged peak postglacial warmth: Molecular evidence in lake sediment from Arctic Canada. *Glob. Change Biol.* **25**, 4244–4256 (2019).
51. I.G. Alsos, D.P. Rijal, D. Ehrich, D.N. Karger, N.G. Yoccoz, P.D. Heintzman, A.G. Brown, Y. Lammers, L. Pellissier, T. Alm, K.A. Bråthen, E. Coissac, M.K.F. Merkel, A. Alberti, F. Denoeud, J. Bakke, PhyloNorway Consortium, Postglacial species arrival and diversity buildup of northern ecosystems took millennia. *Sci. Adv.* **8**, 1-14 (2022).
52. J.H. Raberg, S.E. Crump, G. de Wet, D.J. Harning, G.H. Miller, Á. Geirsdóttir, J. Sepúlveda, BrGDGT lipids in cold regions reflect summer soil temperature and seasonal soil water chemistry. *Geochim. Cosmochim. Acta* **369**, 111-125 (2024).
53. W. Xiao, Y. Wang, S. Zhou, L. Hu, H. Yang, Y. Xu, Ubiquitous production of branched glycerol dialkyl glycerol tetraethers (brGDGTs) in global marine environments: a new source indicator for brGDGTs. *Biogeosciences* **13**, 5883-5894 (2016).
54. C. Martin, G. Ménot, N. Thouvenay, N. Davtian, V. Andrieu-Ponel, M. Reille, E. Bard, Impact of human activities and vegetation changes on the tetraether sources in Lake St Front (Massif Central, France). *Org. Geochem.* **135**, 38-52 (2019).
55. P.D. Zander, D. Böhl, F. Sirocko, A. Auderset, G.H. Haug, A. Martínez-García, Reconstruction of warm-season temperatures in central Europe during the past 60000 years from lacustrine branched glycerol dialkyl glycerol tetraethers (brGDGTs). *Clim. Past* **20**, 841-864 (2024).

56. Y. Yao, J. Zhao, R.S. Vachula, J.P. Werne, J. Wu, X. Song, Y. Huang, Correlation between the ratio of 5-methyl hexamethylated to pentamethylated branched GDGTs (HP5) and water depth reflects redox variations in stratified lakes. *Org. Geochem.* **147**, 104076 (2020).
57. J. Wu, H. Yang, R.D. Pancost, B.D.A. Naafs, S. Qian, X. Dang, H. Sun, H. Pei, R. Wang, S. Zhao, S. Xie, Variations in dissolved O_2 in a Chinese lake drive changes in microbial communities and impact sedimentary GDGT distributions. *Chem. Geol.* **579**, 120348 (2021).
58. J.M. Russell, E.C. Hopmans, S.E. Loomis, J. Liang, J.S. Sinninghe Damsté, Distributions of 5- and 6-methyl branched glycerol dialkyl glycerol tetraethers (brGDGTs) in East African lake sediment: effects of temperature, pH, and new lacustrine paleotemperature calibrations. *Org. Geochem.* **117**, 56-69 (2018).
59. B. Zhao, I.S. Castañeda, R.S. Bradley, J.M. Salacup, G.A. de Wet, W.C. Daniels, T. Schneider, Development of an in situ branched GDGT calibration in Lake 578, southern Greenland. *Org. Geochem.* **152**, 104168 (2021).
60. F. Ajallooeian, L. Deng, M.A. Lever, C. De Jonge, Seasonal temperature dependency of aquatic branched glycerol dialkyl glycerol tetraethers: A mesocosm approach. *Org. Geochem.* **189**, 104742 (2024)
61. H.J.B. Birks, V.A. Felde, A.E. Bjune, J.-A. Grytnes, H. Seppä, T. Giesecke, Does pollen-assemblage richness reflect floristic richness? A review of recent developments and future challenges. *Rev. Palaeobot. Palynol.* **228**, 1-25 (2016).
62. L. Karlsdóttir, M. Hallsdóttir, Ó. Eggertsson, Æ.Th. Thórsson, K. Anamthawat-Jónsson, Birch hybridization in Thistilfjördur, North-east Iceland during the Holocene. *Icelandic Agricultural Sciences* **27**, 95-109 (2014).
63. N. Roy, N. Bhiry, J. Woollett, B. Fréchette, Vegetation history since the mid-Holocene in northeastern Iceland. *Écoscience* **25**, 109-123 (2018).
64. P. Cabedo-Sanz, S.T. Belt, A.E. Jennings, J.T. Andrews, Á. Geirsdóttir, Á. Variability in drift ice export from the Arctic Ocean to the North Icelandic Shelf over the last 8000 years: A multi-proxy evaluation. *Quat. Sci. Rev.* **146**, 99-115 (2016).
65. D.J. Harning, A.E. Jennings, D. Köseoğlu, S.T. Belt, Á. Geirsdóttir, J. Sepúlveda, Response of biological productivity to North Atlantic marine front migration during the Holocene. *Clim. Past* **17**, 379-396 (2021).
66. L. Sha, K.L. Knudsen, J. Eiríksson, S. Björck, H. Jiang, X. Yang, X. Yu, D. Li, Diatom-reconstructed summer sea-surface temperatures and climatic events off Norh Iceland during the last deglaciation and Holocene. *Palaeogeogr., Palaeoclimatol., Palaeoecol.* **602**, 111154 (2022).
67. N. Roy, J. Woollett, N. Bhiry, G. Haemmerli, V. Forbes, R. Pienitz, Perspectives of landscape change following early settlement (landnám) in Svalbarðstunga, northeastern Iceland. *Boreas* **47**, 671-686 (2018).
68. J. Raberg, D. Harning, Á. Geirsdóttir, J. Sepúlveda, G.H. Miller, Soil and lake water temperatures of Iceland (2019-2021). Arctic Data Center [data set], http://doi.org/10.18739/A2XP6V46R (2021).
69. G. Larsen, S. Thorarinsson, H4 and other acid Hekla tephra layers. *Jökull* **27**, 28-46 (1977).
70. M. Blaauw, J.A. Christen, Flexible paleoclimate age-depth models using an autoregressive gamma process. *Bayesian Anal.* **6**, 457–474 (2011).
71. P.J. Reimer, W.E.N., Austin, E. Bard, A. Bayliss, P.G. Blackwell, C. Bronk Ramsey, M. Butzin, H. Cheng, R.L. Edwards, M. Friedrich, P.M. Grootes, T.P. Guilderson, I. Hajdas, T.J. Heaton, A.G. Hogg, K.A. Hughen, B. Kromer, S.W. Manning, R. Muscheler, J.G. Palmer, C. Pearson, J. van der Plicht, R.W. Reimer, D.A. Richards, E.M. Scott, J.R. Southon, C.S.M. Turney, L. Wacker, F. Adolphi, U. Büntgen, M. Capano, S.M. Fahri, A. Fogtmann-Schulz, R. Friedrich, P. Köhler, S. Kudsk, F. Miyake, J. Olsen, F. Reinig, M. Sakamoto, A. Sookdeo, S.

Talamo, S., The IntCal20 northern hemisphere radiocarbon age calibration curve (0-55 cal kBP). *Radiocarbon*, **62**, 725-757 (2020).
72. C. Huguet, E.C. Hopmans, W. Febo-Ayala, D.H. Thompson, J.S. Sinninghe Damsté, S. Schouten, An improved method to determine the absolute abundance of glycerol dibiphytanyl glycerol tetraether lipids. *Org. Geochem.* **37**, 1036–1041 (2006).
73. E.C. Hopmans, S. Schouten, J.S. Sinninghe Damsté, The effect of improved chromatography on GDGT-based palaeoproxies. *Org. Geochem.* **93**, 1–6 (2016).
74. M.D. O'Beirne, W.P. Scott, J.P. Werne, A critical assessment of lacustrine branched glycerol dialkyl glycerol tetraether (brGDGT) temperature calibration models. *Geochim. Cosmochim. Acta* **359**, 100-118 (2023).
75. W.J. D'Andrea, S. Theroux, R.S. Bradley, X. Huang, Does phylogeny control U^{K}_{37}-temperature sensitivity? Implications for lacustrine alkenone paleothermometry. *Geochim. Cosmochim. Acta* **175**, 168–180 (2016).
76. N. Rohland, I. Glocke, A. Aximu-Petri, M. Meyer, Extraction of highly degraded DNA from ancient bones, teeth and sediments for high-throughout sequencing. *Nat. Protoc.* **13**, 2447-2461 (2018).
77. F.V. Seersholm, D.J. Werndly, A. Grealy, T. Johnson, E.M.K. Early, E.L.Jr. Lundelius, B. Winsborough, G.E. Farr, R. Toomey, A.J. Hansen, B. Shapiro, M.R. Waters, G. McDonald, A. Linderholm, T.W.Jr. Stafford, M. Bunce, Rapid range shifts and megafaunal extinctions associated with late Pleistocene climate change. *Nat. Comm.* **11**, 1-10, 2020.
78. T.J. Murchie, M. Kuch, A.T. Duggan, L. Ledger, K. Roche, J. Klunk, E. Karpinski, D. Hackenberger, T. Sadoway, R. MacPhee, D. Froese, H. Poinar, Optimizing extraction and targeted capture of ancient environmental DNA for reconstructing past environments using the PalaeoChip Arctic-1.0 bait-set. *Quat. Res.* **99**, 305–328 (2021).
79. J.D. Kapp, R.E. Green, B. Shapiro, A fast and efficient single-stranded genomic library preparation method optimized for ancient DNA. *J. Hered.* **112**, 241–249 (2021).
80. V. Slon, I. Glocke, R. Barkai, A. Gopher, I. Hershkovitz, M. Meyer, Mammalian mitochondrial capture, a tool for rapid screening of DNA preservation in faunal and undiagnostic remains, and its application to Middle Pleistocene specimens from Qesem Cave (Israel). *Quat. Int.* **398**, 210–218 (2016).
81. T.L. Fulton, B. Shapiro, Setting Up an Ancient DNA Laboratory. In: Shapiro, B., Barlow, A., Heintzman, P., Hofreiter, M., Paijmans, J., Soares, A. (eds) Ancient DNA. Methods in Molecular Biology, vol 1963. Humana Press, New York, NY (2019).
82. P.J. McMurdie, S. Holmes, phyloseq: An R package for reproducible interactive analysis and graphics of microbiome census data. *PLoS ONE* **8**, e61217 (2013).
83. E.E. Curd, Z. Gold, G.S. Kandlikar, J. Gomer, M. Ogden, T. O'Connell, L. Pipes, T.M. Schweizer, L. Rabichow, M. Lin, B. Shi, P.H. Barber, N. Kraft, R. Wayne, R.S. Meyer, *Anacapa Toolkit*: An environmental DNA toolkit for processing multilocus metabarcode datasets. *Methods Ecol. Evol.* **10**, 1469-1475 (2019).
84. J.H. Sønstebø, L. Gielly, A.K. Brysting, R. Elven, M. Edwards, J. Haile, E. Willerslev, E. Coissac, D. Rioux, J. Sannier, P. Taberlet, C. Brochmann, Using next-generation sequencing for molecular reconstruction of past Arctic vegetation and climate. *Mol. Ecol. Res.* **10**, 1009-1018 (2010).
85. G.J. Hannon, FASTX-Toolkit. http://hannonlab.cshl.edu/fastx_toolkit (2010).
86. B.J. Callahan, P.J. McMurdie, M.J. Rosen, A.W. Han, A.J.A. Johnson, S.P. Holmes, DADA2: High-resolution sample inference from Illumina amplicon data. *Nat. Methods* **13**, 581-583 (2016).
87. B. Langmead, S.L. Salzberg, Fast gapped-read alignment with Bowtie 2. *Nature Meth.* **9**, 357-359 (2012).

88. R Core Team, R: A language and environment for statistical computing. Vienna, Austria: R Foundation for Statistical Computing, https://www.R-project.org/ (2021).

Acknowledgments

We kindly thank Sveinbjörn Steinþórsson and Þór Blöndahl for lake coring assistance, Prof. Thomas Marchitto for access to the Trace Metal Lab, and Brooke Holman, Isiah Castro, and Dr. Nadia Dildar for lab assistance.

Funding: National Science Foundation ARCSS #1836981 (GHM, ÁG, and JS)

Author contributions: Funding acquisition and Supervision: ÁG, GHM, JS, and BS. Investigation: DJH, SS, JHR, NA, ÁG, and GHM. Visualization: DJH. Writing (original draft): DJH. Writing (review and editing): SS, JHR, NA, JS, BS, GHM, and ÁG.

Competing interests: Authors declare that they have no competing interests.

Data and materials availability: Data associated with this manuscript has been submitted to the NOAA NCEI Paleoclimatology database and will be available there upon final publication.